ACCSCIENCE PUBLISHING

Asian Journal of Water, Environment and Pollution

ORIGINAL RESEARCH ARTICLE

Comparative study on the CO_2 capture performance of sludge pyrolysis biochar prepared with different inorganic dehydrating conditioners

Yingjie Huang[1†], Yuexin Zhang[1,2†], Rui Dong[1], Jianfeng Fang[1], Yizhou Li[1], Yang Yang[1], Tianfeng Tang[3], and Jiangdi Deng[1,4*]

[1]Three Gorges Reservoir Area Environment and Ecology of Chongqing Observation and Research Station, Chongqing Three Gorges University, Wan Zhou, Chongqing, China

[2]Emergency Environmental Bureau of the Industrial Park, Cuiping District, Yibin, Sichuan, China

[3]Chongqing Liangping District Ecological Environment Bureau, Liangping, Chongqing, China

[4]Chongqing GreenKarbon Environmental Protection Technology Co., Ltd., Chongqing, China

Abstract

To address the limited understanding of how inorganic dehydrating conditioners affect the CO_2 capture performance of sludge-derived biochar, this study investigated three representative conditioners: polyferric chloride, polyferric sulfate (PFS), and polyaluminosilicate ferric salt, and evaluated their influence on biochar properties and carbon dioxide (CO_2) adsorption. The effects of conditioner dosage were first optimized, and two preparation routes, conventional *ex situ* pyrolysis and cyclic pyrolysis, were then compared. The resulting biochars were systematically characterized, and their adsorption behavior was analyzed using physicochemical characterization and adsorption kinetics modeling to elucidate the synergistic roles of conditioner type and pyrolysis mode. The results show that the biochar prepared from PFS-conditioned sludge by cyclic pyrolysis (SS-PFS cycle) exhibited the best performance at the optimal dosage ratio, achieving a CO_2 adsorption capacity of 101.48 mg/g at 25 °C. Mechanistic analysis revealed that the SS-PFS cycle possessed a more developed pore structure, a richer surface functional group density, and a higher carbon defect density, all of which synergistically enhanced both physical and chemical adsorption of CO_2. After 10 consecutive adsorption–desorption cycles, the material retained 58.94% of its initial adsorption capacity, indicating reasonable reusability. These findings confirm that combining PFS conditioning with cyclic pyrolysis is a viable strategy for improving the CO_2 capture performance of sludge-derived biochar and provide both theoretical support and technical guidance for the high-value utilization of sewage sludge.

Keywords: Sludge; Biochar; CO_2 capture; Pyrolysis; Inorganic dehydrating conditioners

1. Introduction

The expansion of wastewater treatment infrastructure has led to a corresponding increase in global sewage sludge production.[1] Effective sludge dewatering is a prerequisite for

†*These authors contributed equally to this work.*

***Corresponding author:**
Jiangdi Deng
(Dengjd.cn@gmail.com)

Citation: Huang Y, Zhang Y, Dong R, *et al.* Comparative study on the CO_2 capture performance of sludge pyrolysis biochar prepared with different inorganic dehydrating conditioners. *Asian J Water Environ Pollut.* 2026;23(4):026120081. doi: 10.36922/AJWEP026120081

Received: March 20, 2026

Revised: April 23, 2026

Accepted: May 6, 2026

Published online: June 24, 2026

economical transport and safe disposal and is therefore a key step in sustainable sludge management. Chemical coagulation/flocculation is one of the most widely used methods for sludge treatment.[2] It improves solid-liquid separation and dewatering through adsorption, bridging, and charge neutralization, and is simple, efficient, and easy to operate.[2,3]

Chemical flocculants are generally classified as either organic or inorganic. Organic flocculants mainly include polyacrylamide and its derivatives. These materials have high molecular weight, strong bridging ability, and can rapidly form coarse flocs, which significantly improve sludge dewatering efficiency and reduce the dosage of flocculants; however, they are relatively expensive, may introduce environmental risks through organic residues, and can affect the structure and performance of biochar during subsequent sludge pyrolysis. Inorganic flocculants, represented by iron salts, aluminum salts, and their polymers, such as polyferric chloride (PFC), polyferric sulfate (PFS), and polyaluminosilicate ferric salt (PSAF), promote sludge-floc aggregation through electrical double-layer compression and neutralization of the negative surface charge.[4]

Although inorganic flocculants have a relatively weak bridging effect and may require higher dosage under high organic load sludge conditions, these agents are typically low-cost, environmentally compatible, and stable in performance. Compared with organic flocculants, the inorganic residues retained in sludge cake, including iron (Fe), aluminum (Al), and silicon (Si), are less likely to cause secondary pollution during pyrolysis and may even catalyze pyrolysis reactions, regulate the microstructure of biochar, and alter its surface chemistry.[5]

Specifically, Fe and Al species in inorganic conditioners can act as heterogeneous catalysts during pyrolysis, promoting the cracking of macromolecular organic matter in sludge, reducing tar formation, and facilitating pore development in biochar.[6,7] Si-containing components can serve as templates to regulate pore-size distribution and enhance the thermal stability of the biochar framework.[8] These effects create opportunities for the high-value utilization of sludge-derived biochar.

Biochar has been widely studied as a promising carbon dioxide (CO_2) adsorbent due to its low cost, adjustable structure, and good stability. Studies have shown that biomass-derived biochar, sludge-based biochar, and activated biochar all exhibit strong CO_2 adsorption performance at ambient temperature, under flue gas conditions, and under cyclic utilization conditions.[9] The CO_2 adsorption capacity of biochar is closely related to its specific surface area, pore structure, surface functional groups, and heteroatom doping, which can be regulated by raw material composition, preparation method, and modification conditions.[10]

Polyferric sulfate, PFC, and PSAF are commonly used inorganic conditioners in sludge dewatering. PFC can significantly increase sludge particle size and form a loose floc structure, often giving better dewatering performance than conventional ferric chloride; PSAF is a silica-Al–Fe composite inorganic polymer coagulant. Using sodium silicate as a carrier and coagulant aid, it can form a compact network structure with higher molecular weight and stronger bridging ability through the synergistic action of silicate, iron, and aluminum species, thereby improving sludge dewatering.[11] This type of complex conditioner is also considered environmentally friendly and cost-effective.[12] In addition, previous studies suggest that aminosilanes and metal elements such as Fe, Si, and Al can improve the CO_2 capture capacity of biochar by modifying its surface properties.[6,13,14] Fe-containing conditioners may also promote pyrolysis reactions and optimize the adsorption properties of the resulting biochar.[7]

Among the sludge resource-utilization technologies developed in recent years, sludge pyrolysis has attracted increasing attention because it offers simultaneous reduction, harmless treatment, and resource recovery.[15] This process can retain more than 50% of the carbon originally present in dewatered sludge, thereby contributing to carbon-peaking and carbon-neutrality goals.[16] Sludge catalytic pyrolysis is currently a major development direction in this field.[17] According to the interaction mode between the raw material and catalyst, catalytic pyrolysis can be broadly divided into *in situ* and *ex situ* configurations. In *in situ* catalytic pyrolysis, pyrolysis and catalytic reactions occur in the same reactor. Although this arrangement is simple, it may suffer from insufficient contact between pyrolysis vapor and catalyst and from coke accumulation on the catalyst surface, both of which gradually reduce catalytic activity.[18] In *ex situ* catalytic pyrolysis, the pyrolysis and catalytic reforming stages are separated, improving contact between volatile products and the catalyst by optimizing reaction conditions.[18,19] However, the residence time of pyrolysis vapor in conventional *ex situ* catalytic systems remains relatively short, and the conversion of complex compounds, such as tar, remains limited.[20]

To address these limitations, a newly developed cyclic pyrolysis system incorporates an extended external circulation–heating section. This design increases the residence time of pyrolysis vapors, promotes more complete decomposition of organic intermediates, reduces the formation of complex tar compounds, and improves the yield and quality of both biochar and pyrolysis gas.[21]

Preliminary single-factor experiments indicated that sludge biochar prepared by cyclic catalytic pyrolysis had a higher yield, a larger pore structure, richer surface functional groups, and more stable chemical properties than biochar produced by the conventional *ex situ* process, and consequently displayed better adsorption performance.[21,22] However, because inorganic conditioners used during dewatering remain in the sludge cake and enter the pyrolysis stage, they can alter the microstructure, surface chemistry, and mineral composition of the resulting biochar, thereby influencing its CO_2 capture performance.[23] Although sludge-derived biochar has been widely studied for CO_2 adsorption, the specific effects of inorganic conditioners remain poorly understood, and the different mechanisms associated with Fe salts and silica–Al–Fe composite salts are still unclear.

Therefore, this study selected three typical inorganic conditioners, namely PFS, PFC, and PSAF, to systematically investigate their effects on the CO_2 capture performance of sludge-derived biochar within the sludge conditioning–dewatering–pyrolysis chain. By optimizing conditioner dosage, comparing conventional *ex situ* pyrolysis with cyclic pyrolysis, and correlating physicochemical characterization with adsorption kinetics analysis, this work clarifies the underlying mechanisms and provides theoretical and technical support for selecting dewatering conditioners that improve the CO_2 capture performance of sludge-derived biochar.

2. Materials and methods

2.1. Experimental materials

Sludge samples were collected from the Xintian town municipal wastewater treatment plant in Xintian town, Wanzhou district, Chongqing, China. The plant adopts the oxidation ditch process and has a design capacity of 0.3 million m^3/d of wastewater. After collection, the sludge was allowed to stand for 2 h, the supernatant was removed, and the sludge was stored in polyethylene containers at 4 °C for no longer than 1 week before use. Prior to each experiment, the sludge was equilibrated in a 20 °C water bath for 30 min to maintain sample consistency and to preserve its representativeness relative to the *in situ* residual activated sludge in the treatment plant. The inorganic conditioners used in this study were PFC, PSAF, and PFS. PFC was purchased from Henan Jinxuyuan Environmental Protection Science and Technology Co., Ltd. (China), whereas PSAF and PFS were purchased from Henan Shiyuan Water Purification Material Co. (China). The main properties of the raw sludge are listed in Table 1.

2.2. Sludge conditioning and dewatering

The dosage of PFC, PSAF, and PFS was expressed as grams of conditioner per kilogram of dry sludge (g/kg DS), with test levels of 0, 40, 80, 120, 160, and 200 g/kg DS. Each conditioner was prepared as a five wt% aqueous solution and allowed to stand for five min after complete dissolution.

For each test, 500 mL of sludge was transferred into a 1 L beaker. A predetermined amount of conditioner was added, followed by rapid mixing at 350 revolutions per minute (r/min) for 30 s and then slow mixing at 40 r/min for 3 min. After conditioning, the sludge was filtered using a Büchner funnel connected to a circulating-water vacuum pump with a qualitative filter paper of 11 μm pore size. The resulting sludge cake was dried at 105 ± 5 °C for at least 8 h to constant weight, and the mass loss before and after drying was used to calculate the moisture content. For the blank control, no conditioner was added. Finally, all dewatered sludge cakes were ground, passed through a 100-mesh sieve (particle size ≤ 0.15 mm), and sealed for subsequent experiments.

2.3. Evaluation of sludge dewatering performance

The main indicators used to evaluate sludge dewatering performance were specific resistance to filtration (SRF), filter-cake moisture content (FCM), and sludge settling ratio (SV_{30}). Detailed procedures are provided in Supplementary S1.

2.4. Conventional *ex situ* pyrolysis and cyclic pyrolysis systems

The conventional *ex situ* pyrolysis system consists of (i) an N_2 cylinder, (ii) a pyrolysis unit, (iii) a catalytic unit, (iv) a temperature-control system, (v) a condensation system, and (vi) a gas-collection unit (Figure 1A). In this configuration, pyrolysis vapors flow in one direction through the system, resulting in a relatively short residence time. The cyclic pyrolysis system includes two additional components compared with the conventional system: (vii)

Table 1. Industrial analysis of sludge samples

Moisture content	Mineral content	Volatile matter	Fixed carbon	Organic matter
98.96%	21.97%	77.40%	0.64%	21.31%

a motor speed regulator, and (viii) an externally heated gas-circulation loop[22] (Figure 1B). This design allows the pyrolysis vapors generated in the sludge-pyrolysis section to recirculate within the reactor, extending vapor residence time and improving vapor decomposition.

2.5. Preparation of sludge biochar

The dried and ground sludge samples obtained after conditioning were pyrolyzed at 600 °C. According to our preliminary experiments and previous studies,[21,22] 600 °C was selected because sludge biochar achieves a balance among high carbon retention, developed pore structure, and suitable surface functional groups, which favors CO_2 adsorption; lower temperatures lead to incomplete pyrolysis and underdeveloped pores, while higher temperatures cause excessive carbon loss and pore collapse.

For the conventional *ex situ* pyrolysis route, 2 g of sludge was placed in a quartz boat and introduced into a tube furnace. Before heating, the furnace was purged with N_2 for 10 min. The temperature was then increased to 600 °C under N_2 at a heating rate of 10 °C/min and held for 1 h to ensure complete pyrolysis of organic matter and full catalytic effect of inorganic conditioners, according to the optimized parameters reported in the literature.[24] A continuous N_2 flow was maintained during cooling, and the biochar was collected after the furnace cooled to room temperature.

For cyclic pyrolysis, 2 g of the sludge sample was placed in a quartz boat and introduced into the designated section of the cyclic pyrolysis unit. The motor speed was fixed at 1050 r/min under sealed conditions.[22] Air in the system was removed by purging with N_2 for 15 min, after which the sludge was pyrolyzed at 600 °C. The pyrolysis, catalytic reforming, and external recirculation sections were maintained at the same final temperature for 1 h. After cooling, the biochar was collected and stored in sealed, dry containers.

The biochars prepared by the conventional *ex situ* pyrolysis route were denoted as follows: SS ordinary (raw sludge biochar), SS-PFC ordinary, SS-PSAF ordinary, and SS-PFS ordinary. The biochars prepared by cyclic pyrolysis were denoted as SS cycle, SS-PFC cycle, SS-PSAF cycle, and SS-PFS cycle.

2.6. Carbon dioxide adsorption by sludge biochar

Approximately 5 mg of biochar was pretreated at 120 °C under N_2 for 40 min to remove moisture and volatiles. After cooling naturally to the target adsorption temperature (25, 30, 75, or 105 °C), CO_2 adsorption was carried out at a gas flow rate of 50 mL/min for 60 min. The adsorption capacity of CO_2 was used as the main index to determine the optimal adsorption temperature.

2.7. Characterization of physicochemical properties

Thermogravimetric analysis and differential scanning

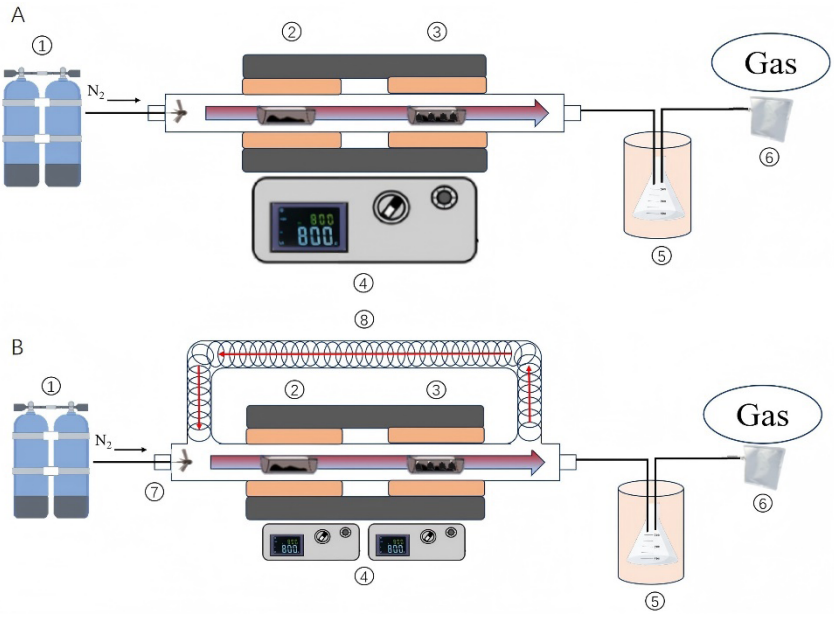

Figure 1. Schematic diagrams of pyrolysis units: (A) Normal *ex situ* pyrolysis unit, (B) Cyclic *ex situ* pyrolysis unit

calorimetry (TG-DSC; STA449F3, Netzsch, Germany) were used to evaluate CO_2 adsorption behavior and kinetics. Surface area and pore-size distribution were measured using an Autosorb-iQ2 automatic specific-surface-area analyzer (Quantachrome Instruments, United States of America [USA]). Surface functional groups were characterized by Fourier transform infrared spectroscopy (FTIR; Nicolet iS50, Thermo Fisher, USA), morphology was observed by scanning electron microscopy (SEM; SU3500, Hitachi, Japan), crystallinity was analyzed by X-ray diffraction (XRD; D8 Advance, Bruker, Germany), and carbon structure and phase composition were further investigated by Raman spectroscopy (LabRAM HR Evolution, HORIBA, France) and X-ray photoelectron spectroscopy (XPS; ESCALAB 250Xi, Thermo Fisher, USA).

2.8. Analysis of carbon dioxide adsorption data

The CO_2 adsorption data were calculated using the adsorption equations and fitted with adsorption kinetics models. The specific equations and calculation methods are as follows:

(i) CO_2 adsorption by biochar

The adsorption of biochar for CO_2 was calculated as in **Equation 1**:

$$Q = \frac{q_{1-}q_2}{q_1} \times 1000 \quad (1)$$

In the formula: Q is the adsorption amount of biochar (mg/g);

q_1 is the initial weight of biochar (mg);

q_2 is the weight of the biochar after CO_2 adsorption (mg)

(ii) Fitting the kinetic model

A quasi-primary kinetic model (**Equation 2**), a quasi-secondary kinetic model (**Equation 3**), and an Avrami model (**Equation 4**) were used to fit the adsorption data.[25]

$$q_1 = q_e\left(1 - e^{\frac{-k_1 t}{2.303}}\right) \quad (2)$$

$$q_1 = \frac{k_2 t q_e^2}{1 + k_2 t q_e} \quad (3)$$

$$q_t = q_e\left(1 - e^{-(kt)^n}\right) \quad (4)$$

In the formula: q_t is the CO_2 content adsorbed by biochar at time t (mg/g);

q_e is the amount of CO_2 adsorbed by the biochar when adsorption reaches equilibrium (mg/g);

t is the time of CO_2 adsorption by biochar;

k_1 is the quasi-primary kinetic constant; k_2 is the quasi-secondary kinetic constant;

k, n are the relevant adsorption rate constants.

2.9. Cyclic adsorption–desorption experiments

To evaluate regeneration performance, 10 adsorption–desorption cycles were carried out using the optimal conditioner type, the optimal biochar-preparation system, and the optimal adsorption temperature identified in the single-cycle experiments. In each cycle, the sample was pretreated as described above, followed by CO_2 adsorption for 1 h and N_2 desorption at 120 °C for 0.5 h with an N_2 flow rate of 100 mL/min.

3. Results and discussion

3.1. Effect of inorganic conditioner dosage on sludge dewaterability

The optimal dosage of PFC was 80 g/kg DS (Figure 2A). The most obvious decrease in SRF occurred when the dosage increased from 0 to 80 g/kg DS, while the slope change became much smaller at higher dosages. At 80 g/kg DS, the FCM also decreased to approximately 87%, indicating improved water removal. Although SV_{30} was not the minimum value at this dosage, it was substantially lower than that of the untreated sludge, indicating improved settling. Because SRF was selected as the primary evaluation index, with FCM and SV_{30} as secondary indices, 80 g/kg DS was considered the optimal PFC dosage.

The initial SRF was approximately 41 × 10^{11} m/kg (Figure 2B). When 40 g/kg DS of PSAF was added, SRF sharply decreased to about 12 × 10^{11} m/kg. Further increases in dosage produced only small additional reductions, and the SRF gradually stabilized by 200 g/kg DS. The FCM also decreased rapidly, reaching approximately 83.5% at 40 g/kg DS, followed by a slight increase at higher dosages. The SV_{30} initially decreased and then increased, reaching its minimum at approximately 120 g/kg DS. Given the sharp improvement in SRF and the low FCM observed at 40 g/kg DS, the optimal PSAF dosage was identified as 40 g/kg DS.

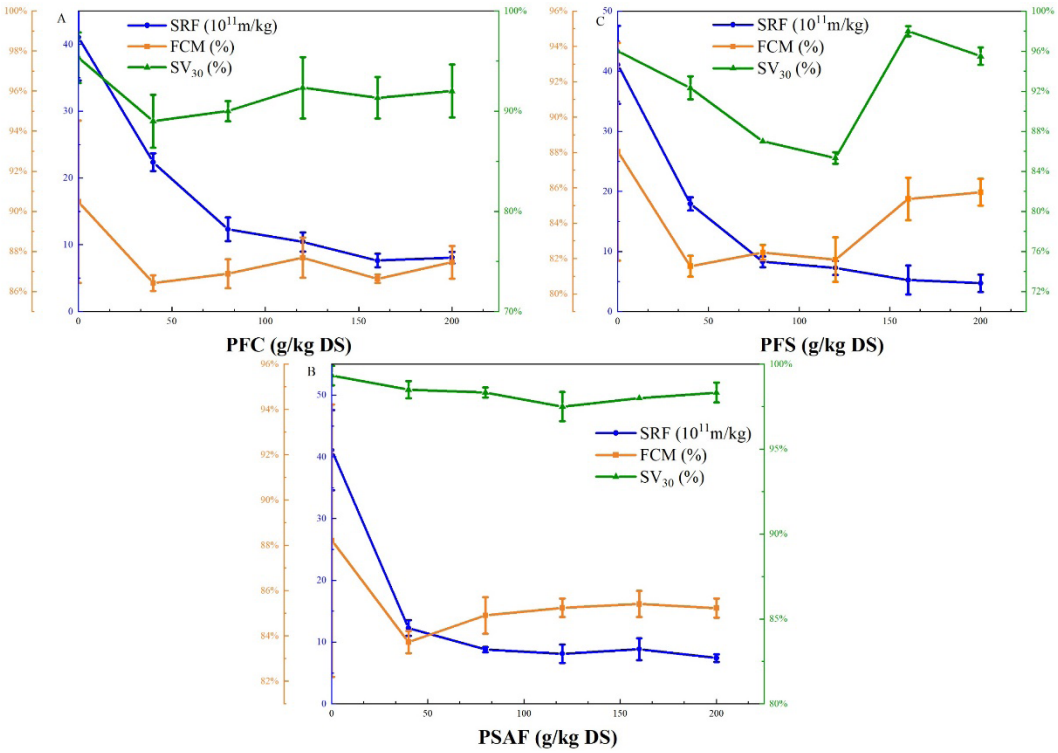

Figure 2. Trend of evaluation indicators at different dosages of inorganic conditioners (indicators separated, samples together): (A) polyferric chloride (PFC), (B) polyaluminosilicate ferric salt (PSAF), (C) polyferric sulfate (PFS)
Abbreviations: SRF: Specific resistance to filtration; FCM: Filter-cake moisture content; SV_{30}: Sludge settling ratio.

When the PFS dosage reached 40 g/kg DS, SRF decreased to about 17×10^{11} m/kg (Figure 2C). At higher dosages, the rate of decrease became much smaller and the SRF gradually stabilized by 200 g/kg DS. This indicates that PFS was particularly effective in the early stage of sludge conditioning. The FCM decreased rapidly, reaching a minimum of approximately 81.5% at 40 g/kg DS. SV_{30} first decreased and then increased, reaching a favorable value at around 120 g/kg DS. SV_{30} increases at excessive dosages due to charge over-neutralization and particle restabilization, and the small standard deviations confirm good experimental repeatability. Considering the overall balance among SRF, FCM, and SV_{30}, with SRF as the primary dewatering index, the optimal dosage was determined at the inflection point of the SRF curve; the optimal PFS dosage was set at 80 g/kg DS.

The optimal dosages of PFC (80 g/kg DS), PSAF (40 g/kg DS), and PFS (80 g/kg DS) are consistent with reported ranges for inorganic sludge conditioners.[8] PSAF shows the lowest optimal dosage due to the Si–Al–Fe synergistic effect, which agrees with the high efficiency of composite coagulants.[11]

Overall, systematic optimization based on SRF, FCM, and SV_{30} identified optimal dosages of 80 g/kg DS for PFC, 40 g/kg DS for PSAF, and 80 g/kg DS for PFS. All optimal dosages were determined primarily based on the SRF turning point, the key indicator of sludge dewaterability. Both PFC and PFS significantly reduced SRF at similar dosages, indicating efficient improvement of sludge dewaterability through charge neutralization and double-layer compression. PSAF required the lowest dosage, suggesting that its silica–Al–Fe synergistic effect strengthened floc structure and reduced chemical demand.

3.2. Comparative effects of pyrolysis methods on carbon dioxide adsorption by sludge-derived biochar

For biochars prepared by conventional *ex situ* pyrolysis, the CO_2 adsorption capacities of SS, SS-PFC, SS-PSAF, and SS-PFS at different adsorption temperatures were compared (Figure 3A–3D). SS showed its highest adsorption capacity at 30 °C, with an equilibrium adsorption capacity of approximately 73.35 mg/g. SS-PFC showed its best performance at 25 °C, with an equilibrium adsorption capacity of approximately 79.71 mg/g, slightly higher than

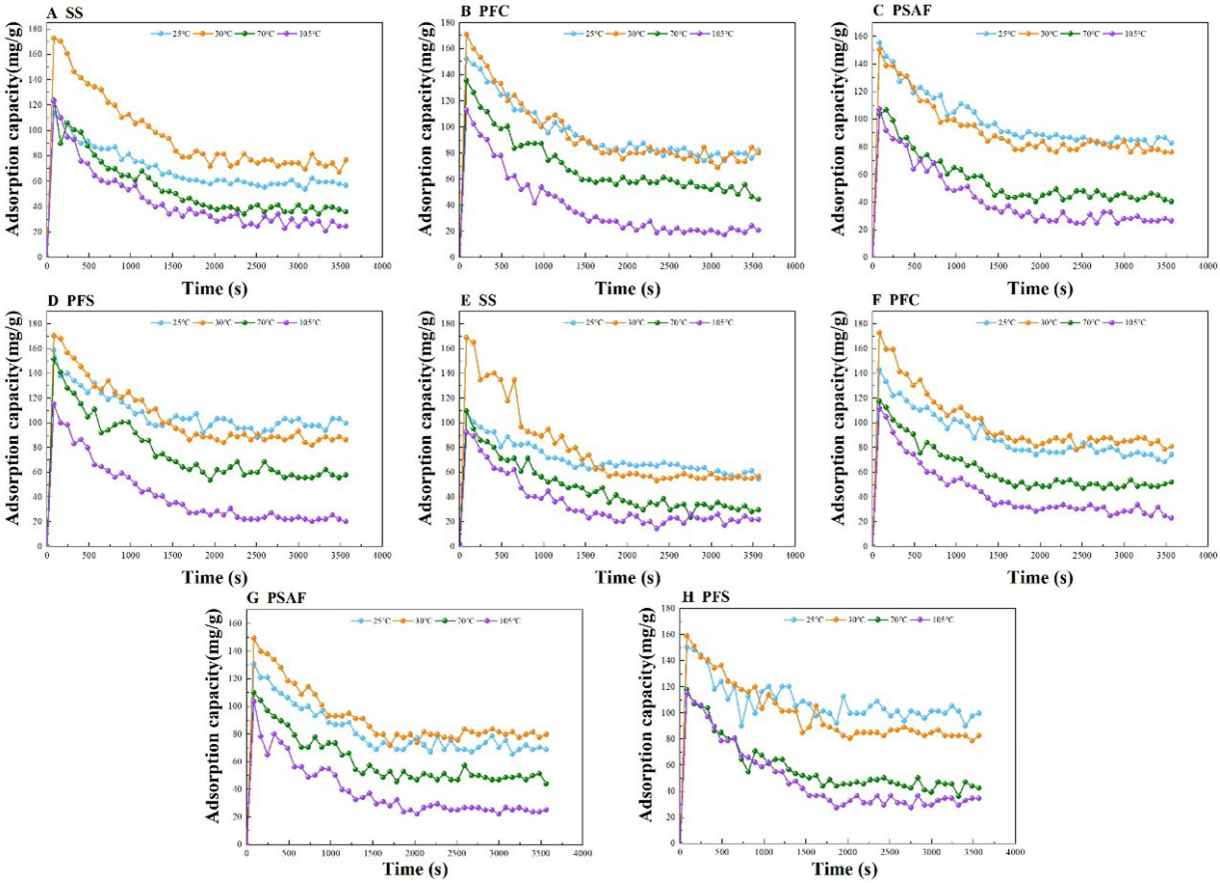

Figure 3. Carbon dioxide (CO_2) adsorption curves of sludge biochar with different inorganic conditioners under ordinary and cyclic pyrolysis**.** A–H shows the effect of CO_2 adsorption properties of biochar prepared with different inorganic conditioners under ordinary *ex situ* pyrolysis, respectively. E–H shows the effect of CO_2 adsorption properties of biochar prepared with different inorganic conditioners under cyclic pyrolysis SS. (A) SS, (B) SS-PFC, (C) SS-PSAF, (D) SS-PFS, (E) SS cycle, (F) SS-PFC cycle, (G) SS-PSAF cycle, (H) SS-PFS cycle.
Abbreviations: PFC: Polyferric chloride; PFS: Polyferric sulfate; PSAF: Polyaluminosilicate ferric salt; SS: Raw sludge.

that at 30 °C (76.8 mg/g). SS-PSAF also showed the best adsorption at 25 °C, reaching approximately 85.85 mg/g. Among all conventionally prepared biochars, SS-PFS ordinary performed best, with an equilibrium adsorption capacity of approximately 100.81 mg/g at 25 °C, compared with 90.19 mg/g at 30 °C. Thus, under conventional *ex situ* pyrolysis, the adsorption capacity of conditioned biochars was consistently higher than that of the unconditioned control, with PFS conditioning giving the best result.

Figure 3E–3H compares the adsorption capacities of the corresponding cyclic–pyrolysis biochars. The SS cycle exhibited its highest adsorption capacity at 25 °C, reaching about 60.45 mg/g, which was higher than that at 30 °C (55.61 mg/g). The SS-PFC cycle performed best at 30 °C, reaching about 84.71 mg/g, higher than at 25 °C (75.77 mg/g). SS-PSAF cycle showed its highest adsorption capacity at 25 °C, with an equilibrium adsorption capacity of approximately 79.64 mg/g. SS-PFS cycle exhibited the best overall performance, reaching 101.48 mg/g at 25 °C, which was substantially higher than its capacity at 30 °C (84.7 mg/g). Thus, in the cyclic pyrolysis mode, PFS-conditioned biochar again showed the best CO_2 adsorption performance. Moreover, its adsorption capacity is comparable to, or even exceeds, that of many commercially available biomass biochar materials, such as longan shells (which, according to existing research, exhibit a maximum adsorption capacity of 91.05 mg/g at an optimal adsorption temperature of 25 °C)[26] and coconut shells (which exhibit a maximum adsorption capacity of 82.58 mg/g at an optimal adsorption temperature of 30 °C)[27], demonstrating outstanding adsorption performance.

Based on the above results, the best-performing biochars under the two pyrolysis routes were SS ordinary, SS-PFC cycle, SS-PSAF ordinary, and SS-PFS cycle,

respectively, with SS-PFS cycle exhibiting the highest overall adsorption capacity of 101.48 mg/g (Figure 4). This advantage may be related to the ability of sulfate ions derived from PFS to retain part of the nitrogen in the sludge and to form thermally stable salts with metal ions,[24] as verified by the dense lamellar structure observed in the SEM image of the SS-PFS cycle. Additional XPS Fe2p spectra analysis (Figure S1) confirms the existence of stable Fe-based species (e.g., ferric oxide [Fe_2O_3], Fe–S complexes) in the biochar, which are the key components of the lamellar structure and further support the proposed mechanism. Previous studies also indicate that Fe sulfate can modify biochar surface morphology by inducing the growth of dense lamellar crystals.[28] Such structures may suppress the volatilization of organic matter during pyrolysis and thereby improve adsorption stability. In addition, iron sulfate is relatively inexpensive and has a lower secondary environmental impact than some alternative additives.

3.3. Cyclic adsorption performance

To evaluate regeneration behavior, the SS ordinary and SS-PFS cycles were selected for 10 adsorption–desorption cycles, and the results are shown in Figure 5. In both cases, the CO_2 adsorption capacity gradually decreased with increasing cycle number. For SS ordinary, the adsorption capacity decreased by 48.92%, from 73.34 mg/g to 35.93 mg/g. For the SS-PFS cycle, the capacity decreased by 41.06%, from 101.48 mg/g to 59.87 mg/g. Even after 10 cycles, the SS-PFS cycle retained more than half of its initial adsorption capacity, indicating that it possesses not only high CO_2 adsorption capacity but also acceptable regeneration performance.

3.4. Mechanistic analysis

3.4.1. Kinetic analysis

Three common kinetic models were used to fit the adsorption data: the pseudo-first-order model, which is generally associated with reversible physical adsorption; the pseudo-second-order model, which is commonly used to describe chemisorption involving bond formation between adsorbent and adsorbate; and the Avrami model, which has been widely applied to adsorption processes influenced by both physical and chemical interactions[29]. As shown in Table 2, the predicted adsorption capacities of the biochars were close to the experimental values, and all three models gave high correlation coefficients (R^2), indicating that CO_2 adsorption on these biochars involves both physical and chemical interactions.[30]

3.4.2. Morphological and pore-structure analysis

To characterize structural properties, the optimal biochars

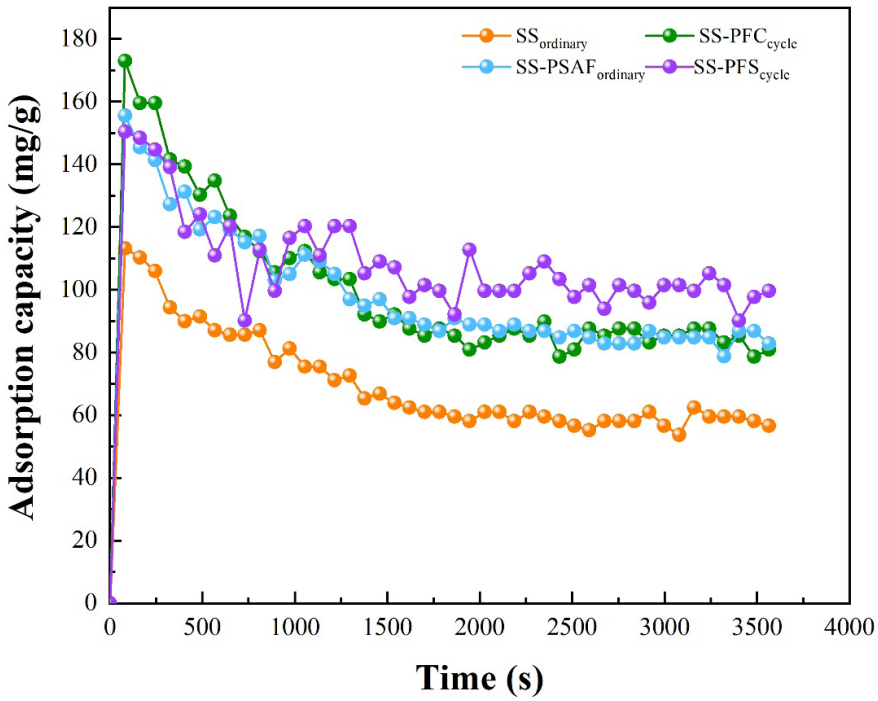

Figure 4. Comparison of optimum adsorption temperatures for different pyrolysis methods
Abbreviations: PFC: Polyferric chloride; PFS: Polyferric sulfate; PSAF: Polyaluminosilicate ferric salt; SS: Raw sludge.

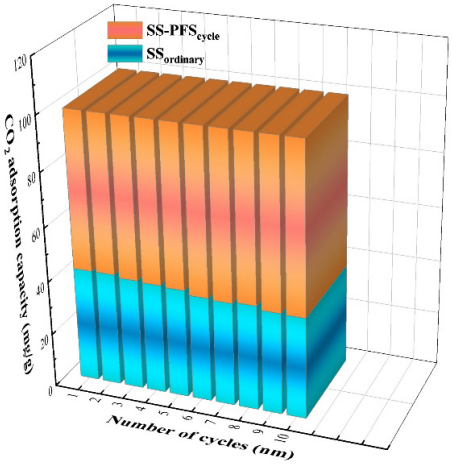

Figure 5. Biochar recycling performance
Abbreviations: CO_2: Carbon dioxide; PFS: Polyferric sulfate; SS: Raw sludge.

Table 2. Parameters of adsorption kinetic model

Biochar	Pseudo-first-order model		Pseudo-secondary-order model		Avrami model		
	k_1	R^2	k_1	R^2	k	n	R^2
SS$_{ordinary}$	0.0602	0.935	0.0018	0.976	0.0722	1.24	0.987
SS-PFC$_{cycle}$	0.0680	0.875	0.0019	0.850	0.0693	1.19	0.986
SS-PSAF$_{ordinary}$	0.0587	0.867	0.0019	0.749	0.0615	1.14	0.956
SS-PFS$_{cycle}$	0.0783	0.962	0.0021	0.985	0.049	1.12	0.985

Abbreviations: PFC: Polyferric chloride; PFS: Polyferric sulfate; PSAF: Polyaluminosilicate ferric salt; SS: Raw sludge.

prepared from raw sludge and from sludge conditioned with different inorganic agents were analyzed by SEM and the Brunauer–Emmett–Teller method (ASAP 246, Micromeritics, USA). Figure 6 shows the SEM images. The irregular pores and heterogeneous pore distribution observed in the SS ordinary can be attributed to the complex composition of the sludge feedstock. SS-PFC cycle showed a predominantly lumpy structure with a rough surface, which may include incompletely decomposed organic matter or mineral particles. SS-PSAF ordinary exhibited a porous, but relatively disordered, structure, likely due to the release of volatile components during pyrolysis. In contrast, the SS-PFS cycle produced a denser, more uniformly distributed pore structure than the other biochars. This structure increases the contact area between biochar and CO_2, thereby improving adsorption capacity. Iron sulfate modification may promote the formation of micro- and mesopores through catalytic or templating effects of the metal salt.[31] The surface may also be covered with iron-containing derivatives, such as Fe_2O_3 or magnetite, resulting in more regular crystal structures or attached nanoparticles.[32]

The structural parameters shown in Figure 6 further demonstrate that conditioner addition altered specific surface area, total pore volume, and average pore diameter. Compared with the ordinary SS, the highest specific surface areas were observed for the SS-PFS (15.04 m^2/g) and SS-PFC (14.2 m^2/g) cycles, indicating more complex surface structures and a greater number of available adsorption sites. SS-PFS cycle also showed the largest total pore volume (0.0218 cm^3/g) and a favorable average pore

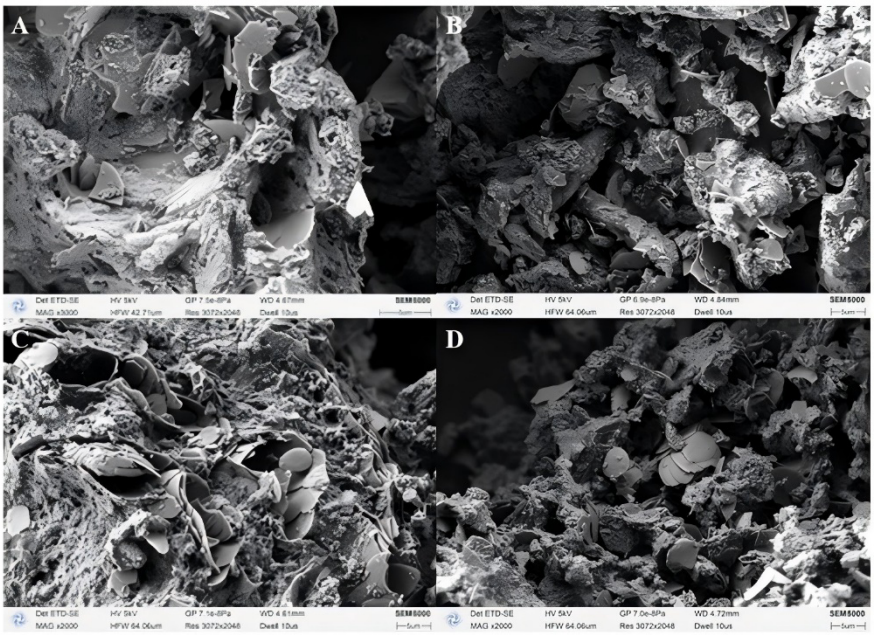

E Samples	Specific surface area (m^2/g)	Total pore volume (cm^3/g)	Average pore size (nm)
SS $_{ordinary}$	12.7268	0.01652	4.7273
SS-PFC $_{cycle}$	14.2014	0.02113	4.887
SS-PSAF $_{ordinary}$	12.4751	0.01821	4.9228
SS-PFS $_{cycle}$	15.0435	0.0218	5.5835

Figure 6. Scanning electron micrographs of biochar: (A) SS $_{ordinary}$, (B) SS-PFC $_{cycle}$, (C) SS-PSAF $_{ordinary}$, (D) SS-PFS $_{cycle}$, (E) biochar structure. Scale bar: 5 μm. Magnification: (A) 3,000×, (B–D) 2,000×.
Abbreviations: PFC: Polyferric chloride; PFS: Polyferric sulfate; PSAF: Polyaluminosilicate ferric salt; SS: Raw sludge.

diameter (5.58 nm), indicating a more developed internal pore network with greater capacity to accommodate and store CO_2 molecules. These pore-structure advantages collectively contributed to enhanced adsorption performance. The crystalline phases of the biochar samples are presented in Supplementary S5.

3.4.3. Surface functional group

Fourier transform infrared spectroscopy was used to characterize surface functional groups in the different biochars. The spectra of the ordinary and conditioned biochars before adsorption are shown in Figure 7. Multiple absorption peaks were observed,[33–35] including peaks assigned to C–N (1,027 cm^{-1}), C=O (1,652 cm^{-1}), C–H (around 3,908 cm^{-1}), C–S (536 cm^{-1}), and N–H/O–H stretching (3,462 cm^{-1}).[36] The spectra of conditioned biochars differed noticeably from that of the unconditioned biochar. In the 3,462–3,968 cm^{-1} region, the SS-PSAF ordinary and SS-PFS cycle showed pronounced differences, with the SS-PFS cycle displaying a stronger absorption peak, suggesting a higher abundance of oxygen-containing functional groups and more active adsorption sites for CO_2. This may be attributed to both the retention of nitrogen-containing species after PFS conditioning and to the more complete reactions enabled by cyclic pyrolysis, which prolongs the interaction time between sludge-derived intermediates and catalyst residues. As a result, oxygen- and nitrogen-containing active sites have more opportunity to form and remain on the biochar surface. The stronger peak above 3,462 cm^{-1} also indicates an increase in nitrogen-containing surface groups in the SS-PFS cycle, which may further promote CO_2 adsorption.[37] The relatively small changes in the 3,000–600 cm^{-1} region suggest that oxygen-containing functional groups play a particularly important role in the chemisorption contribution of the SS-PFS cycle.

The main peaks of biochar corresponding to C, N, and O were observed near 282, 396, and 529 eV (Figure

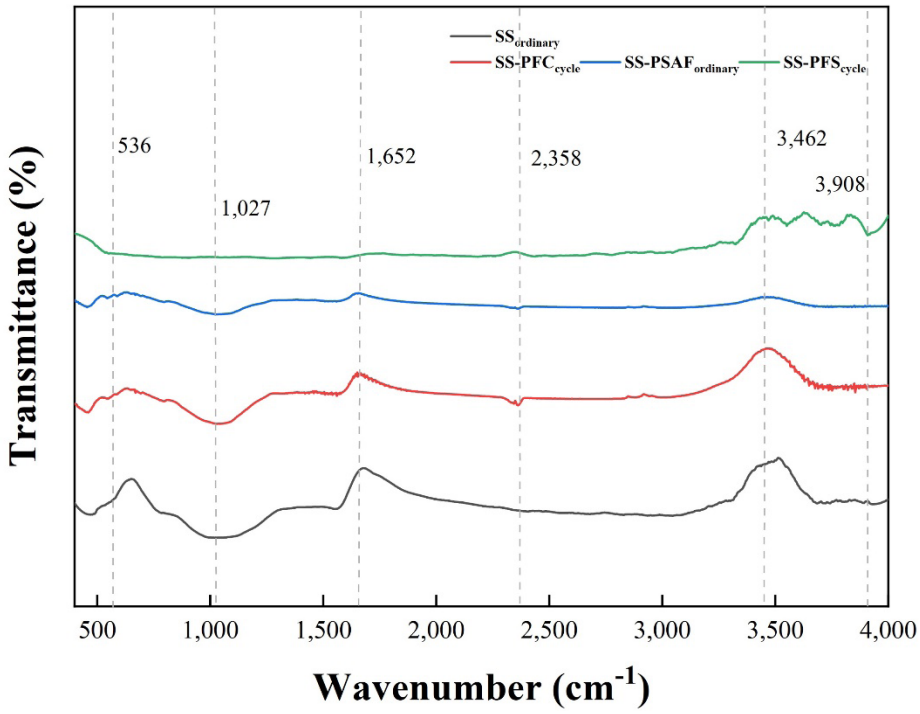

Figure 7. Fourier transform infrared spectra of biochar
Abbreviations: PFC: Polyferric chloride; PFS: Polyferric sulfate; PSAF: Polyaluminosilicate ferric salt; SS: Raw sludge.

8), respectively. The main peaks corresponding to C, N, and O appeared near 282, 396, and 529 eV, respectively. Conditioner addition altered the relative contents of C, N, and O, although carbon and oxygen remained the dominant elements. As shown in Figure 8B, the SS-PFS cycle contained 83.84% carbon and 14.55% oxygen, both of which were relatively high among the tested biochars. A high carbon content can enhance CO_2 adsorption through London dispersion interactions,[38] while oxygen-containing groups can also improve adsorption performance.[9]

The deconvoluted C1s spectra were resolved into peaks corresponding to graphitic sp^2 C–C (284.8 eV), C–O in hydroxyl or ether groups (286.0–286.2 eV), and O=C–O in carboxyl or ester groups (288.6–288.8 eV)[39] (Figure 9). Compared with the SS ordinary (8.5%), the relative content of O=C–O groups in the SS-PFS cycle increased significantly to 18.2%, indicating enrichment of carboxyl-containing groups on the biochar surface. The increase in such groups enhances surface acidity, suggesting that chemisorption contributes to CO_2 uptake in the SS-PFS cycle.

The O1s spectra were deconvoluted into peaks corresponding to C–O–C/O–H groups (532.1–532.3 eV) and C=O groups (533.5–533.7 eV) (Figure 10). Compared with ordinary SS, cycled SS-PFS showed a clear enrichment of C=O groups. These groups can facilitate physical trapping of CO_2 through hydrogen bonding and dipole–dipole interactions and may also coordinate with Fe species introduced by PFS.[40,41] Together, these features enhance the physical adsorption capacity for CO2 and demonstrate that the increase in oxygen-containing surface functional groups during the SS-PFS cycle plays an important role in its superior adsorption behavior.

In summary, the superior CO_2 adsorption performance of the SS-PFS cycle is mainly due to three synergistic effects. First, the Fe-based components introduced by PFS conditioning act as heterogeneous catalysts during cyclic pyrolysis, promoting the cracking of organic matter, inhibiting the formation of dense carbon structures, and increasing carbon defects, thereby providing more physical adsorption sites.[6,7] Second, cyclic pyrolysis prolongs the residence time of volatiles and facilitates the formation of a well-developed pore structure, thereby enhancing the diffusion and physical adsorption of CO_2 molecules.[22] Third, PFS conditioning enriches oxygen-containing functional groups (C=O, O=C–O) on the biochar surface, which can form hydrogen bonds, dipole–dipole interactions, and even weak chemical bonding with CO_2, thus strengthening

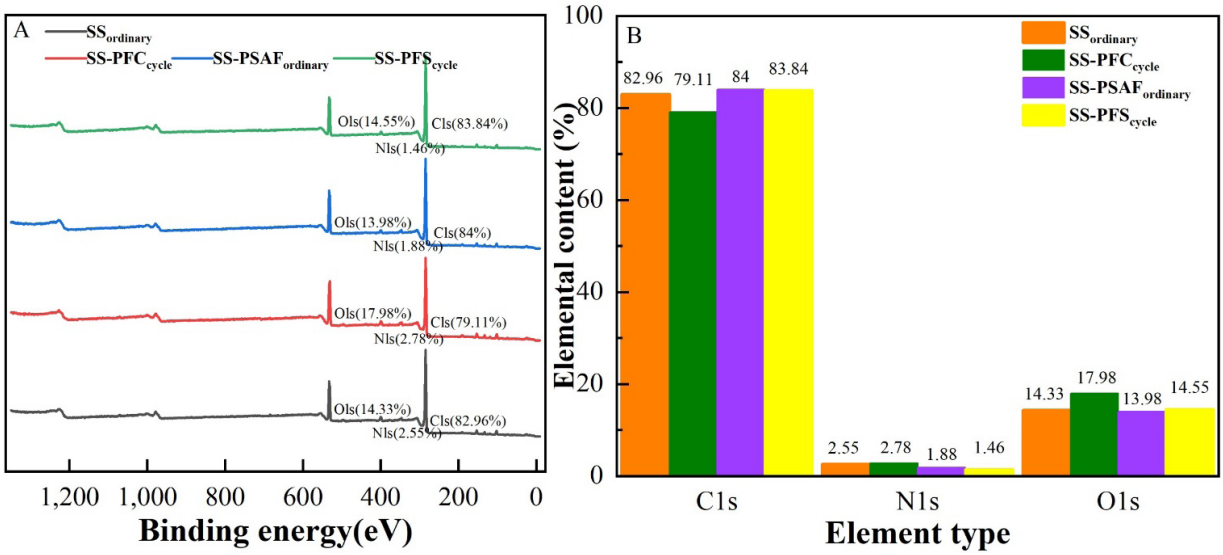

Figure 8. X-ray photoelectron spectra of biochar. (A) Binding energy. (B) Element type.

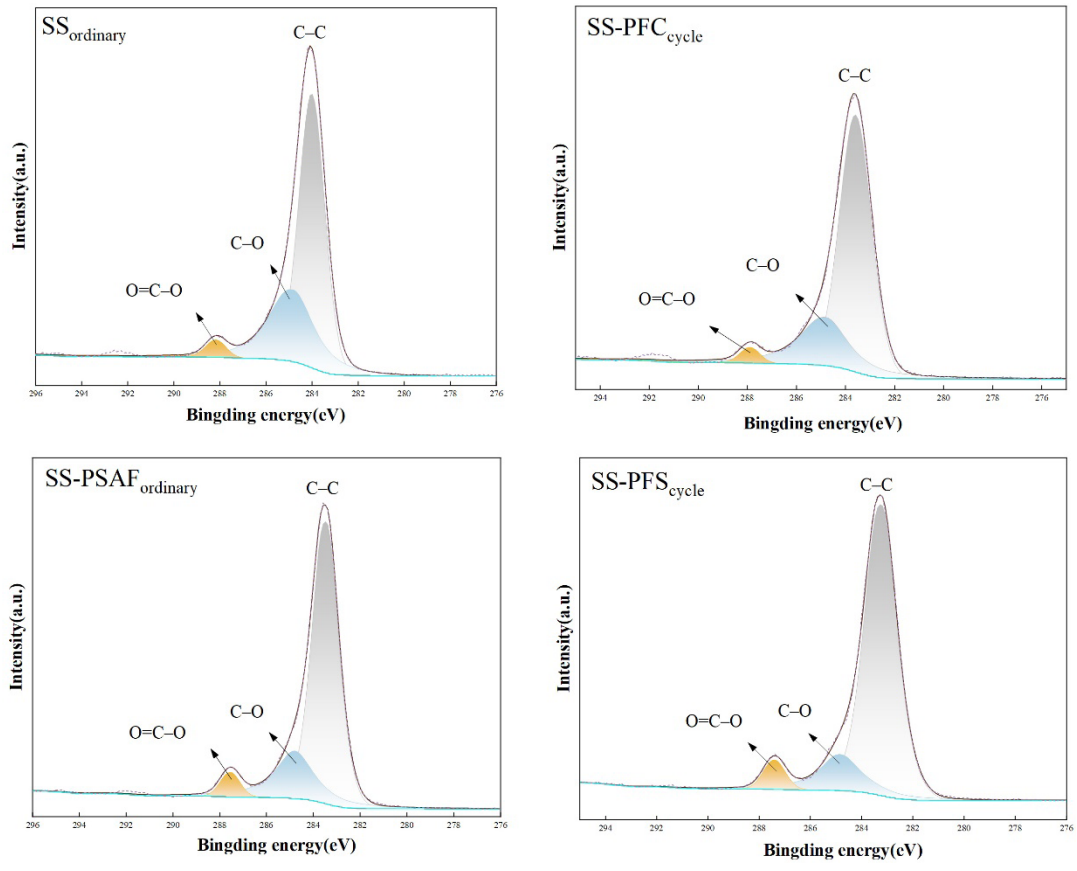

Figure 9. C1s X-ray photoelectron spectroscopy spectra of biochar
Abbreviations: PFC: Polyferric chloride; PFS: Polyferric sulfate; PSAF: Polyaluminosilicate ferric salt; SS: Raw sludge.

chemisorption. The coupling of physical adsorption from defective porous carbon structure and chemical adsorption from surface functional groups collectively contributes to the highest CO_2 uptake of the SS-PFS cycle.

3.4.4. Carbon-structure characterization

The Raman spectra of the biochars showed two major bands corresponding to the D band near 1,350 cm^{-1}, associated with carbon lattice defects, and the G band near 1,580 cm^{-1} (Figure 11), assigned to the in-plane vibration of the sp^2 carbon atom.[42,43] The ID/IG ratio is commonly used as an indicator of graphitization degree, with a higher ratio indicating a greater abundance of defects and disorder.[44] The ID/IG ratio increased significantly to

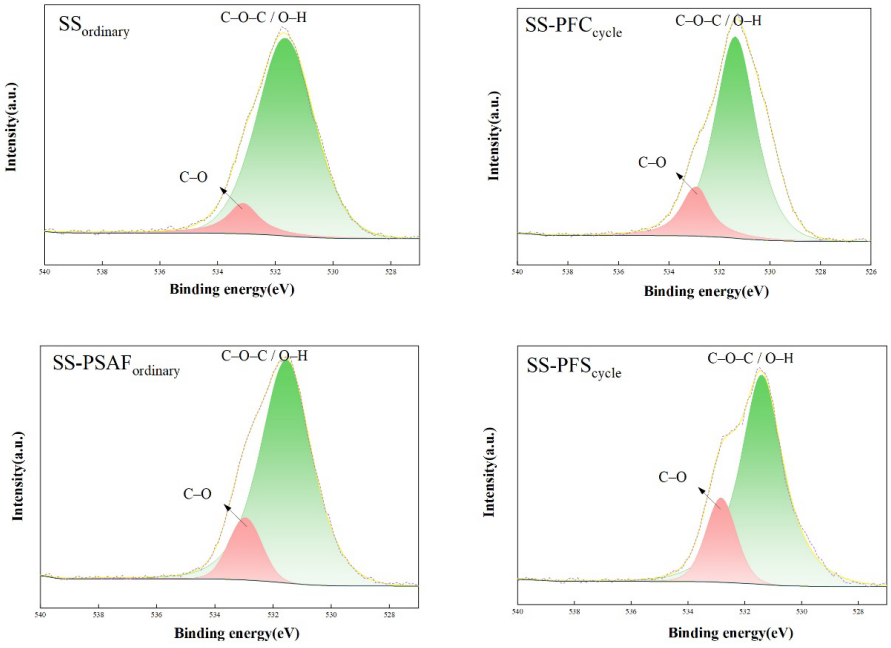

Figure 10. O1s X-ray photoelectron spectroscopy spectra of biochar
Abbreviations: PFC: Polyferric chloride; PFS: Polyferric sulfate; PSAF: Polyaluminosilicate ferric salt; SS: Raw sludge.

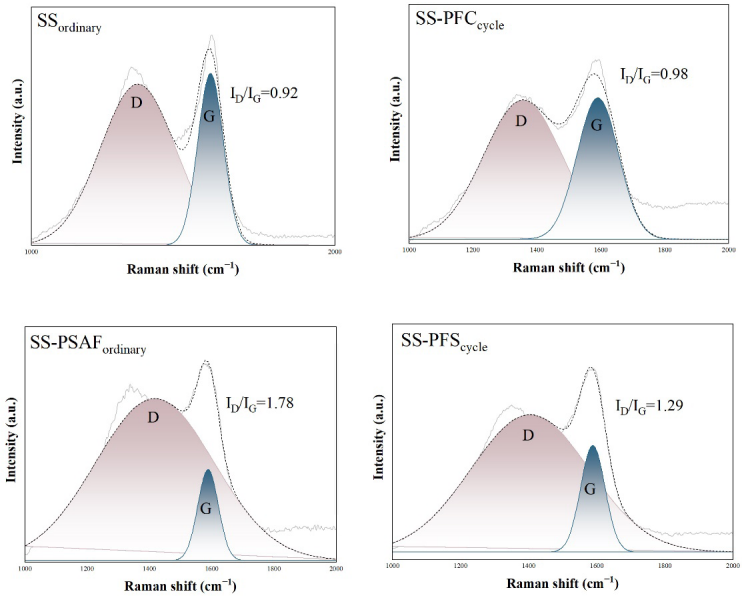

Figure 11. Raman spectra of biochar
Abbreviations: PFC: Polyferric chloride; PFS: Polyferric sulfate; PSAF: Polyaluminosilicate ferric salt; SS: Raw sludge.

1.29 in the SS-PFS cycle compared with the SS ordinary. This result indicates that PFS modification combined with cyclic pyrolysis increased the defect density in the carbon skeleton and reduced the degree of graphitization. Such a highly defective, disordered carbon structure provides more physical adsorption sites, thereby favoring CO_2 capture.[45] Moreover, the catalytic effect of PFS is sustained during the cyclic process, and the longer reaction time allows more complete interaction between conditioner residues and the carbon matrix, further hindering the formation of highly ordered graphitic structures. Therefore, the adsorption of CO_2 by the SS-PFS cycle includes an important physisorption contribution. However, the elevated ID/IG ratio alone cannot explain the full performance. When considered together with the XPS results in Figures 9 and 10, the Raman data indicate that chemisorption associated with oxygen-containing functional groups, such as carboxyl and carbonyl groups, also contributes significantly. Thus, the excellent CO_2 adsorption performance of the SS-PFS cycle results from the combined effects of enhanced physisorption on defective carbon structures and chemisorption on abundant surface functional groups.

4. Conclusion

This study compared the effects of three inorganic dewatering conditioners (PFC, PFS, and PSAF) on sludge dewatering and on the CO_2 adsorption performance of sludge-derived biochar. By establishing a multi-index dewatering evaluation system, the optimal dosages of the conditioners were identified. Among the biochars prepared at 600 °C, the PFS-conditioned biochar produced by cyclic pyrolysis (SS-PFS cycle) exhibited the best CO_2 adsorption performance, reaching 101.48 mg/g at 25 °C. SS-PFS cycle also showed acceptable regeneration stability, retaining 58.94% of its initial adsorption capacity after 10 adsorption-desorption cycles.

The enhanced performance of the SS-PFS cycle is attributed to the combined contributions of physical and chemical adsorption. In particular, the material exhibited a more developed pore structure, a greater density of surface functional groups, and a higher density of carbon defects than the other tested biochars. These results indicate that PFS-conditioned sludge biochar prepared by cyclic pyrolysis has strong potential for CO2 capture, and that selecting an appropriate dewatering conditioner is critical for promoting the utilization of sludge resources.

This technology integrates sludge disposal and CO_2 capture, consistent with waste reduction, recycling, and low-carbon development. Inorganic conditioners are low-cost and readily available; the cyclic pyrolysis system is scalable; and the biochar shows stable recyclability, demonstrating high engineering feasibility. This provides a new technical route for low-carbon utilization of municipal sludge.

Future work should further optimize CO_2 adsorption conditions, investigate the influence of pyrolysis temperature on the adsorption behavior of the SS-PFS cycle, and explore the synergistic effects of mixed conditioners and conditioner formulations on the structure and adsorption performance of sludge-derived biochar.

Acknowledgments

None.

Funding

This work was supported by the National Natural Science Foundation of China (grant number 51808089) and the Science and Technology Research Program of Chongqing Municipal Education Commission (Grant No. KJZD-M202501203).

Conflict of interest

The authors declare that they have no competing interests.

Author contributions

Conceptualization: Yingjie Huang, Yuexin Zhang, Jiangdi Deng
Formal analysis: Rui Dong, Yang Yang
Investigation: Jianfeng Fang, Yizhou Li
Methodology: Tianfeng Tang
Writing–original draft: Yingjie Huang, Yuexin Zhang
Writing–review & editing: Jiangdi Deng

Availability of data

Data are available from the corresponding author upon reasonable request.

References

1. Chen R, Dai X, Dong B. Decrease the effective temperature of hydrothermal treatment for sewage sludge deep dewatering: mechanistic of tannic acid aided. *Water Res.* 2022;217:118450.

   doi: 10.1016/j.watres.2022.118450

2. Wu B, Dai X, Chai X. Critical review on dewatering of sewage sludge: Influential mechanism, conditioning technologies and implications to sludge re-utilizations. *Water Res.* 2020;180:115912.

   doi: 10.1016/j.watres.2020.115912

3. Ai J, Wang Z, Dionysiou DD, et al. Understanding synergistic mechanisms of ferrous iron activated sulfite oxidation and

organic polymer flocculation for enhancing wastewater sludge dewaterability. *Water Res*. 2021;189:116652.

doi: 10.1016/j.watres.2020.116652

4. Yansha Z, Zhe W, Zhenxiang P, et al. Novel thermodynamic mechanisms of co-conditioning with polymeric aluminum chloride and polyacrylamide for improved sludge dewatering: A paradigm shift in the field. *Environ Res*. 2023;234:116420.

doi: 10.1016/j.envres.2023.116420

5. Pan X, Wang M, Wang X, et al. Comparative study on the effect of different dewatering skeleton conditioners on sludge pyrolysis products. *J Environ Chem Eng.* 2021;9(6):106527.

doi: 10.1016/j.jece.2021.106527

6. Lahijani P, Mohammadi M, Mohamed AR. Metal incorporated biochar as a potential adsorbent for high capacity CO_2 capture at ambient condition. *J CO_2 Util.* 2018;26:281-293.

doi: 10.1016/j.jcou.2018.05.018

7. Yu G, Chen D, Arena U, Huang Z, Dai X. Reforming sewage sludge pyrolysis volatile with Fe-embedded char: Minimization of liquid product yield. *Waste Manag.* 2018;73:464-475.

doi: 10.1016/j.wasman.2017.08.004

8. Shaopu L, Yong K. Impacts of key preparation factors on polymerization and flocculation performance of polyferric silicate sulfate (PFSiS). *Colloids Surf A Physicochem Eng Asp.* 2022;635.

doi: 10.1016/j.colsurfa.2021.128109

9. Urooj K, Yop RK, Seul-Yi L, Soo-Jin P. Solvent-free conversion of cucumber peels to N-doped microporous carbons for efficient CO_2 capture performance. *J Clean Prod.* 2022;369:133367.

doi: 10.1016/j.jclepro.2022.133367

10. Chang L, Chuan F, Tingzhen L, et al. CO_2 capture using biochar derived from conditioned sludge via pyrolysis. *Sep Purif Technol.* 2023;314:123624 .

doi: 10.1016/j.seppur.2023.123624

11. Li J, Liu X, Cheng F. Bio-refractory organics removal and floc characteristics of poly-silicic-cation coagulants in tertiary-treatment of coking wastewater. *Chem Eng J.* 2017;324:10-18.

doi: 10.1016/j.cej.2017.04.142

12. Du Z, Gong Z, Qi W, et al. Coagulation performance and floc characteristics of poly-ferric-titanium-silicate-chloride in coking wastewater treatment. *Colloids Surf A Physicochem Eng Asp.* 2022;642:128413.

doi: 10.1016/j.colsurfa.2022.128413

13. Dissanayake PD, Choi SW, Igalavithana AD, et al. Sustainable gasification biochar as a high efficiency adsorbent for CO_2 capture: A facile method to designer biochar fabrication. *Renew Sustain Energy Rev.* 2020;124:109785.

doi: 10.1016/j.rser.2020.109785

14. Li K, Zhang D, Niu X, et al. Insights into CO_2 adsorption on KOH-activated biochars derived from the mixed sewage sludge and pine sawdust. *Sci Total Environ.* 2022;826:154133.

doi: 10.1016/j.scitotenv.2022.154133

15. Ma R, Huang X, Zhou Y, et al. The effects of catalysts on the conversion of organic matter and bio-fuel production in the microwave pyrolysis of sludge at different temperatures. *Bioresour Technol.* 2017;238:616-623.

doi: 10.1016/j.biortech.2017.04.103

16. Wang Y, Cao S, Li J, et al. The predictive value of plasma exosomal lncRNAs/mRNAs in NSCLC patients receiving immunotherapy. *Adv Med Sci.* 2023;68(1):86-93.

doi: 10.1016/j.advms.2023.01.003

17. Yuan Z, Ma W, Zhu N, Zhu Y, Wu S, Lou Z. Identifying the fate of nitrogenous species during sewage sludge pyrolysis via in-situ tracing of protein-sludge inherent components interactions. S*ci Total Environ*. 2023;859:160437.

doi: 10.1016/j.scitotenv.2022.160437

18. Gamliel DP, Du S, Bollas GM, Valla JA. Investigation of in situ and ex situ catalytic pyrolysis of miscanthus× giganteus using a PyGC–MS microsystem and comparison with a bench-scale spouted-bed reactor. *Bioresour Technol.* 2015;191:187-196.

doi: 10.1016/j.biortech.2015.04.129

19. Wan S, Wang Y. A review on ex situ catalytic fast pyrolysis of biomass. *Front Chem Sci Eng.* 2014;8(3):280-294.

doi: 10.1007/s11705-014-1436-8

20. De Andrés JM, Roche E, Narros A, Rodríguez ME. Characterisation of tar from sewage sludge gasification. Influence of gasifying conditions: Temperature, throughput, steam and use of primary catalysts. *Fuel*. 2016;180:116-126.

doi: 10.1016/j.fuel.2016.04.012

21. Pan X, Wu Y, Li T, et al. A study of co-pyrolysis of sewage sludge and rice husk for syngas production based on a cyclic catalytic integrated process system. *Renew Energy* 2023;215:118946.

doi: 10.1016/j.renene.2023.118946

22. Wu Y, Zhang Y, Wang M, et al. Study on the effect of cyclic catalytic pyrolysis on sludge pyrolysis products. *J Environ Chem Eng.* 2024;12(1):111647.

doi: 10.1016/j.jece.2023.111647

23. Wang M, Pan X, Xia Y, et al. Effect of dewatering conditioners on pollutants with nitrogen, sulfur, and chlorine releasing characteristics during sewage sludge pyrolysis. *Fuel.*

2022;307:121834.

doi: 10.1016/j.fuel.2021.121834

24. Lei W, Li TT, Lv NQ, Liu H, Zhang Y, Xi BD. Study on adsorption of lead by biochar prepared from sludge of municipal wastewater treatment plant. In: *Proceedings of the IOP Conference Series: Materials Science and Engineering*. Bristol: IOP Publishing Ltd; 2019;479(1):012007.

doi: 10.1088/1757-899X/479/1/012007

25. Wang J, Guo X. Adsorption kinetic models: Physical meanings, applications, and solving methods. *J Hazard Mater.* 2020;390:122156.

doi: 10.1016/j.jhazmat.2020.122156

26. Wei H, Chen H, Fu N, et al. Excellent electrochemical properties and large CO_2 capture of nitrogen-doped activated porous carbon synthesised from waste longan shells. *Electrochim Acta.* 2017;231:403-411.

doi: 10.1016/j.electacta.2017.01.194

27. Abdeljaoued A, Querejeta N, Durán I, Álvarez-Gutiérrez N, Pevida C, Chahbani MH. Preparation and Evaluation of a Coconut Shell-Based Activated Carbon for CO_2/CH_4 Separation. *Energies*. 2018;11(7):1748.

doi: 10.3390/en11071748

28. Muñoz M, Garrido MA, Gomez-Rico MF, Font R. PCDD/F determination in sewage sludge composting. Influence of aeration and the presence of PCP. *Sci Total Environ.* 2018;616:763-773.

doi: 10.1016/j.scitotenv.2017.10.249

29. Raganati F, Alfe M, Gargiulo V, Chirone R, Ammendola P. Kinetic study and breakthrough analysis of the hybrid physical/chemical CO_2 adsorption/desorption behavior of a magnetite-based sorbent. *Chem Eng J.* 2019;372:526-535.

doi: 10.1016/j.cej.2019.04.165

30. Li H, Tang M, Huang X, Wang L, Liu Q, Lu S. An efficient biochar adsorbent for CO_2 capture: Combined experimental and theoretical study on the promotion mechanism of N-doping. *Chem Eng J.* 2023;466:143095.

doi: 10.1016/j.cej.2023.143095

31. Zhang Y, Wang B, Wang R. Functionally decorated metal–organic frameworks in environmental remediation. *Chem Eng J.* 2023;455:140741.

doi: 10.1016/j.cej.2022.140741

32. Duan L, Li G, Zhang S, Wang H, Zhao Y, Zhang Y. Sulfur-doped photocatalysts with iron-nitrogen coordination bonds by modifying graphitic carbon nitride obtained from ammonium thiocyanate pyrolysis with ferrous sulfate heptahydrate in ethanol. *Opt Mater.* 2021;118:111222.

doi: 10.1016/j.optmat.2021.111222

33. Ding S, Liu Y. Adsorption of CO_2 from flue gas by novel seaweed-based KOH-activated porous biochars. *Fuel*. 2020;260:116382.

doi: 10.1016/j.fuel.2019.116382

34. Wang Y, Yu G, Xie S, Jiang R, Li C, Xing Z. Pyrolysis of food waste digestate residues for biochar: Pyrolytic properties, biochar characterization, and heavy metal behaviours. *Fuel*. 2023;353:129185.

doi: 10.1016/j.fuel.2023.129185

35. Guo T, Zhang Y, Geng Y, et al. Surface oxidation modification of nitrogen doping biochar for enhancing CO_2 adsorption. *Ind Crops Prod.* 2023;206:117582.

doi: 10.1016/j.indcrop.2023.117582

36. Singh G, Kim IY, Lakhi KS, Srivastava P, Naidu R, Vinu A. Single step synthesis of activated bio-carbons with a high surface area and their excellent CO_2 adsorption capacity. *Carbon*. 2017;116:448-455.

doi: 10.1016/j.carbon.2017.02.015

37. Chen J, Yang J, Hu G, et al. Enhanced CO_2 capture capacity of nitrogen-doped biomass-derived porous carbons. *ACS Sustain Chem Eng.* 2016;4(3):1439-1445.

doi: 10.1021/acssuschemeng.5b01425

38. Rashidi NA, Yusup S, Hameed BH. Kinetic studies on carbon dioxide capture using lignocellulosic based activated carbon. *Energy*. 2013;61:440-446.

doi: 10.1016/j.energy.2013.08.050

39. Tien H-W, Huang Y-L, Yang S-Y, Wang J-Y, Ma C-CM. The production of graphene nanosheets decorated with silver nanoparticles for use in transparent, conductive films. *Carbon*. 2011;49(5):1550-1560.

doi: 10.1016/j.carbon.2010.12.022

40. Latham KG, Dose WM, Allen JA, Donne SW. Nitrogen doped heat treated and activated hydrothermal carbon: NEXAFS examination of the carbon surface at different temperatures. *Carbon*. 2018;128:179-190.

doi: 10.1016/j.carbon.2017.11.072

41. Mahmoudi G, Garcia-Santos I, Safin DA, et al. A joint action of coordination, hydrogen and tetrel bonds toward a new 2D coordination polymer of lead (II) perchlorate and N'-isonicotinoylpyrazine-2-carbohydrazonamide. *Inorg Chem Commun.* 2025;174:113914.

doi: 10.1016/j.inoche.2025.113914

42. Cui Z, Xu G, Ormeci B, Liu H, Zhang Z. Transformation and stabilization of heavy metals during pyrolysis of organic and inorganic-dominated sewage sludges and their mechanisms. *Waste Manag*. 2022;150:57-65.

doi: 10.1016/j.wasman.2022.06.023

43. Lu P, Huang Q, Bourtsalas AT, Chi Y, Yan J. Synergistic effects on char and oil produced by the co-pyrolysis of pine wood,

polyethylene and polyvinyl chloride. *Fuel*. 2018;230:359-367.

doi: 10.1016/j.fuel.2018.05.072

44. Li Y, Zhang G, Liu J, Li G, Wang Y. Optimized preparation of multi-matrix activated carbon for CO_2 capture by response surface methodology: The advantages of co-pyrolysis of biomass and plastics. *J Energy Inst*. 2023;111:101415.

doi: 10.1016/j.joei.2023.101415

45. Wang Y, Xiao JF, Wang HZ, Zhang TC, Yuan SJ. Binary doping of nitrogen and phosphorus into porous carbon: A novel di-functional material for enhancing CO_2 capture and super-capacitance. *J Mater Sci Technol*. 2022;99:73-81.

doi: 10.1016/j.jmst.2021.05.035